The Functional Anatomy of the Deep Facial Fat Compartments: A Detailed Imaging-Based Investigation

Sebastian Cotofana, M.D., Ph.D.
Robert H. Gotkin, M.D.
Konstantin Frank, M.D.
Konstantin C. Koban
Stefan Targosinski, M.D.
Jonathan M. Sykes, M.D.
Markus Schlager
Alexander Schlattau, M.D.
Thilo L. Schenck, M.D., Ph.D.

Albany and New York, N.Y.; Sacramento, Calif.; Munich, Germany; Zurich, Switzerland; and Salzburg, Austria

Background: Injection of soft-tissue fillers into the facial fat compartments is frequently performed to ameliorate the signs of facial aging. This study was designed to investigate the functional anatomy of the deep facial fat compartments and to provide information on the effects of injected material in relation to age and gender differences.

Methods: Forty fresh frozen cephalic specimens of 17 male and 23 female Caucasian body donors (mean age, 76.9 ± 13.1 years; mean body mass index, 23.6 ± 5.3 kg/m^2) were investigated. Computed tomographic and magnetic resonance imaging procedures were carried out using colored contrast-enhanced materials with rheologic properties similar to commercially available soft-tissue fillers. Anatomical dissections were performed to guide conclusions.

Results: No statistically significant influences of age or gender were detected in the investigated sample. Increased amounts of injected contrast agent did not correlate with inferior displacement of the material in any of the investigated compartments: deep pyriform, deep medial cheek, deep lateral cheek, deep nasolabial (located within the premaxillary space), and the medial and lateral sub–orbicularis oculi fat.

Conclusions: Increasing volume in the deep midfacial fat compartments did not cause inferior displacement of the injected material. This underscores the role of deep soft-tissue filler injections (i.e., in contact with the bone) in providing support for overlying structures and resulting in anterior projection. (*Plast. Reconstr. Surg.* 143: 53, 2019.)

The number of soft-tissue filler injections to treat the signs of facial aging has increased substantially during the past 16 years. According to a report of the American Society of Plastic Surgeons, there was a 298 percent increase in these treatments between the years 2000 and 2016.[1] The major goal of these minimally invasive procedures is the restoration of volume within the facial fat compartments.[2]

Subcutaneous and deep facial fat compartments have been introduced to the scientific community, and their precise location and boundaries have been continuously adapted since their first description.[3–13] Both computed tomographic[3] and magnetic resonance[14–19] imaging techniques have been used to visualize these fat compartments, to elucidate their role during facial aging and to provide recommendations for safe and long-lasting results for soft-tissue filler procedures.

The muscles of facial expression have been shown to contribute to the formation of boundaries of the deep midfacial fat compartments [i.e., deep pyriform, deep medial cheek, deep lateral cheek, and deep nasolabial (located within the premaxillary space) and the medial and lateral sub–orbicularis oculi fat].[3–13] According to a previous magnetic resonance imaging study, these muscles undergo no significant age-related changes

From the Department of Medical Education, Albany Medical College; private practice; Facial Plastic and Reconstructive Surgery, University of California, Davis Medical Center; the Department for Hand, Plastic and Aesthetic Surgery, Ludwig Maximilian University; the Division of Thoracic Surgery, University Hospital Zurich; and the Department of Radiology, Paracelsus Medical University Salzburg & Nuremberg.
Received for publication January 6, 2018; accepted July 11, 2018.

DOI: 10.1097/PRS.0000000000005080

Disclosure: *None of the authors has any commercial associations or financial disclosures that might pose or create a conflict of interest with the methods applied or the results presented in this article.*

when muscle length, thickness, or volume or fatty infiltration is measured[15]; this indicates a stable location and course of the facial muscles during the aging process. In a computed tomographic imaging study,[3] a constant volume of 1.0 cc was injected into some of the deep facial fat compartments, and an inferior displacement of 1.3 to 2.6 mm was reported when comparing individuals aged 54 to 75 years to those aged 75 to 104 years. Although it is widely accepted that the facial skeleton undergoes significant changes during aging (e.g., changes in facial widths and angles[20–26]), it is still unknown how these effects ultimately influence the overall functional anatomy of the deep midfacial fat compartments.

The objective of the present study was to investigate the functional anatomy of the deep midfacial fat compartments by using computed tomographic and magnetic resonance imaging methodologies combined with subsequent anatomical dissection. The precise anatomical location of the deep fat compartments, their bounding structures, the migratory potential of various amounts of injected contrast material, and any age and/or gender effects on the functional anatomy of these compartments are evaluated.

MATERIALS AND METHODS

Sample

We investigated 40 fresh frozen cephalic specimens from 17 male and 23 female Caucasian body donors with a mean age of 76.9 ± 13.1 years and a mean body mass index of 23.6 ± 5.3 kg/m^2. Specimens were screened and not included in this analysis if previous facial surgery or diseases disrupted the integrity of the facial anatomy. Each body donor had given informed consent while alive for the use of his or her body for medical, scientific, and educational purposes. All aspects of the study conform to the laws of the country where the study was conducted.

Injection Procedure

The deep facial fat compartments investigated in this analysis were the deep pyriform, deep medial cheek, deep lateral cheek, deep nasolabial (located within the premaxillary space), and the medial and lateral sub–orbicularis oculi fat. The injection procedures were transcutaneous (i.e., perpendicular to the skin surface) implantation of colored radiopaque material using a 20-gauge, 70-mm, sharp-tip needle. The injected material consisted of Visipaque (iodixanol, 320 mg/ml; GE Healthcare, Little Chalfont, United Kingdom), Resource ThickenUp Clear (Nestle HealthCare Nutrition GmbH, Vienna, Austria), and commercially available food coloring. The viscoelastic properties were compared (visually and manually) to commercially available soft-tissue fillers to ensure similar rheologic behavior. Different amounts were injected into the targeted compartments irrespective of side, age, or sex.

Radiographic Imaging

Computed tomographic scans were obtained with cadavers in the upright position, using a head rest to simulate the effects of gravity. The following computed tomographic parameters were applied: slice thickness, 0.6 mm; field of view, 200 mm; increment, 0.5 mm; voltage, 140 kV; and current, 400 mA/second (Figs. 1 through 4).

Magnetic resonance scans were obtained with the cadavers in the supine position (because of spatial limitations of the head coil used), with the following magnetic resonance imaging parameters applied: sagittal T1 Vista (field of view, 270 × 270 × 205 mm; voxel size, 0.7 × 0.7 × 0.35 mm with a voxel reconstruction size of 0.352 mm; signal-to-noise ratio, 1.0; echo time, 18 msec; repetition time, 350 msec; 586 slices per data set); and three-dimensional T2-weighted short inversion time inversion recovery (field of view, 270 × 270 × 204 mm; voxel size, 0.9 × 0.9 × 0.45 mm with a voxel reconstruction size of 0.422 mm; signal-to-noise ratio, 1.0; echo time, 308 msec; repetition time, 3000 msec; 454 slices per data set) (Fig. 5).

Anatomical Dissections

Cephalic specimens were dissected after the imaging procedures at the Surgical Course Center (Salzburg, Austria), and dissections were facilitated by the previously injected colored radiopaque material (Figs. 6 through 8).

Analysis Strategy

On three-dimensional reconstructions, the maximal vertical and horizontal extent of each compartment was measured. The precise location was evaluated in a transverse axis in relation to the midline (distance between the midline and the medialmost and lateralmost aspects) and in a longitudinal axis in relation to a horizontal line at the level of the nasion (horizontal nasion level) (Table 1). Vertical measurements were adjusted for midface height, calculated as the distance between the nasion and the base of the nasal spine (as seen on sagittal computed tomographic scans),

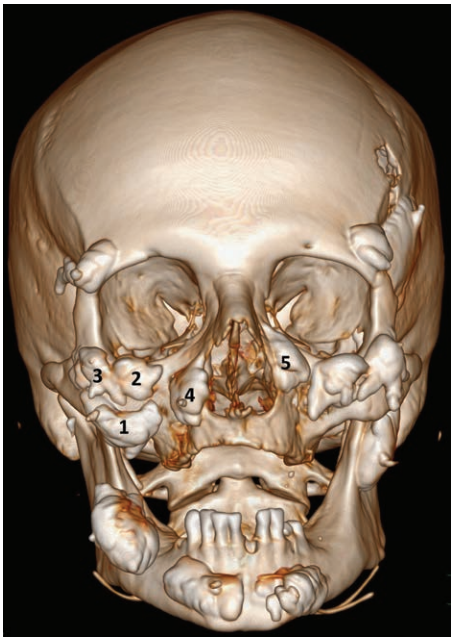

Fig. 1. Three-dimensional reconstruction of contrast-enhanced computed tomographic scan showing the midfacial fat compartments: *1*, deep lateral cheek; *2*, medial suborbicularis oculi; *3*, lateral suborbicularis oculi; *4*, deep pyriform; and *5*, deep nasolabial (located within the premaxillary space). Note that the deep medial cheek fat pad was not contrasted in this scan.

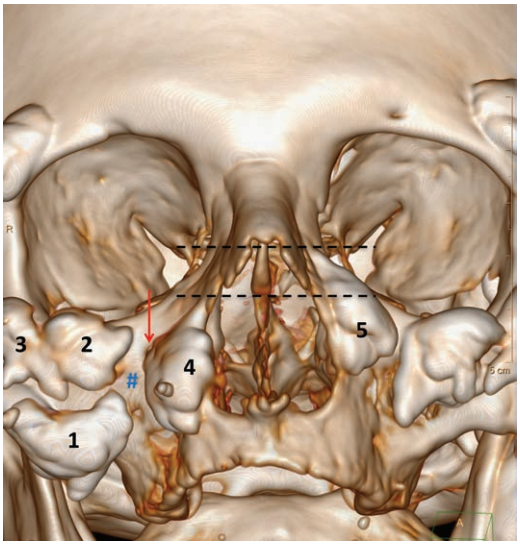

Fig. 2. Three-dimensional reconstruction of contrast-enhanced computed tomographic scan showing the midfacial fat compartments: *1*, deep lateral cheek; *2*, medial suborbicularis oculi; *3*, lateral suborbicularis oculi; *4*, deep pyriform; and *5*, deep nasolabial (located within the premaxillary space). The location of the infraorbital foramen is indicated by the *red arrow*. Note that the deep medial cheek fat was not contrasted in this scan; original location is indicated by the *blue hash*. The difference in superior extent of the deep nasolabial as compared to the deep pyriform compartment is indicated by the *dotted lines*, representing the difference in location above (*5*) and below (*4*) the levator labii superiors alaeque nasi muscle.

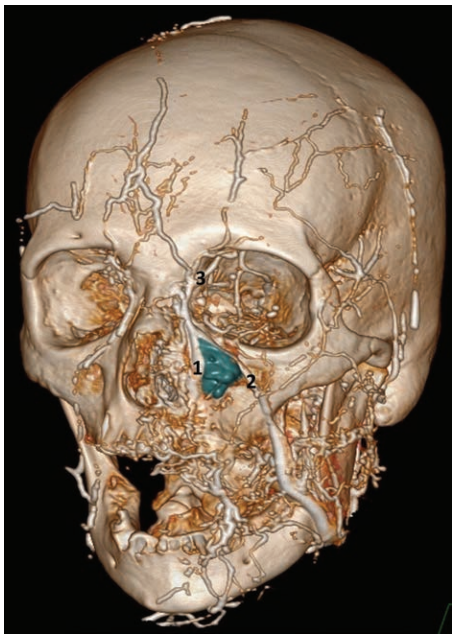

Fig. 3. Three-dimensional reconstruction of contrast-enhanced computed tomographic scan showing the deep nasolabial fat (located within the premaxillary space) in *blue*. The angular vein (*2*) forms the lateral boundary, whereas the lateral nasal vein forms the medial boundary (*1*). Both veins have connections to the superior ophthalmic vein (*3*).

Fig. 4. Three-dimensional reconstruction of contrast-enhanced computed tomographic scan showing the deep pyriform space (*1*) and the deep medial cheek fat (*2*). *Red arrows* indicate the angular artery. Note that on the right side the angular artery travels within the deep pyriform space, whereas on the left side the artery courses medial to the deep medial cheek fat and is thus visible.

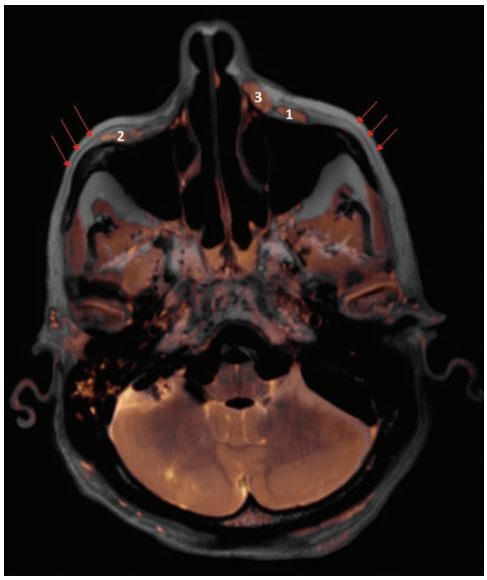

Fig. 5. Fused T1- and T2-weighted magnetic resonance imaging sequences showing the deep medial cheek fat (*1*), the deep lateral cheek fat (*2*), and the deep pyriform space (*3*). *Red arrows* show the orbicularis oculi muscle/midcheek superficial musculoaponeurotic system, providing evidence to the deep location of the deep midfacial fat compartments.

and horizontal measurements were adjusted for the transverse diameter of the cranium calculated at its maximal extent (as seen on transverse computed tomographic scans). Correlations between the amount of the injected volume and the adjusted inferior boundary of each of the investigated compartments were calculated using bivariate correlation models (Pearson, r_p). To also adjust for influences of age and body mass index, generalized linear models were performed using IBM SPSS Version 23 (IBM Corp., Armonk, N.Y.). Results were considered statistically significant at a probability level of $p \leq 0.05$ to guide conclusions.

RESULTS

In the investigated sample (n = 40), female individuals were of lower weight (63.5 ± 16.0 kg versus 81.6 ± 13.0 kg) and had a smaller midface height (75.3 ± 3.0 mm versus 82.0 ± 3.9 mm) compared to men (all $p < 0.001$). Increased age correlated significantly with a lower weight ($r_p = -0.461$; $p < 0.001$) and individuals older than 76 years had a significantly reduced midfacial height (compared to those younger than 76 years): 80.87 ± 6.2 mm versus 77.51 ± 3.1 mm ($p = 0.004$). The inferior margin in any of the investigated compartments showed no significant correlation between increasing amounts of injected "filler" and any inferior displacement of the material (all $p > 0.05$). The superior margin of the deep fat compartments showed no superior displacement if there was a muscular or ligamentous boundary (deep medial cheek, deep lateral cheek, deep pyriform, and medial and lateral sub–orbicularis oculi fat; all $p > 0.05$). An exception was the deep nasolabial

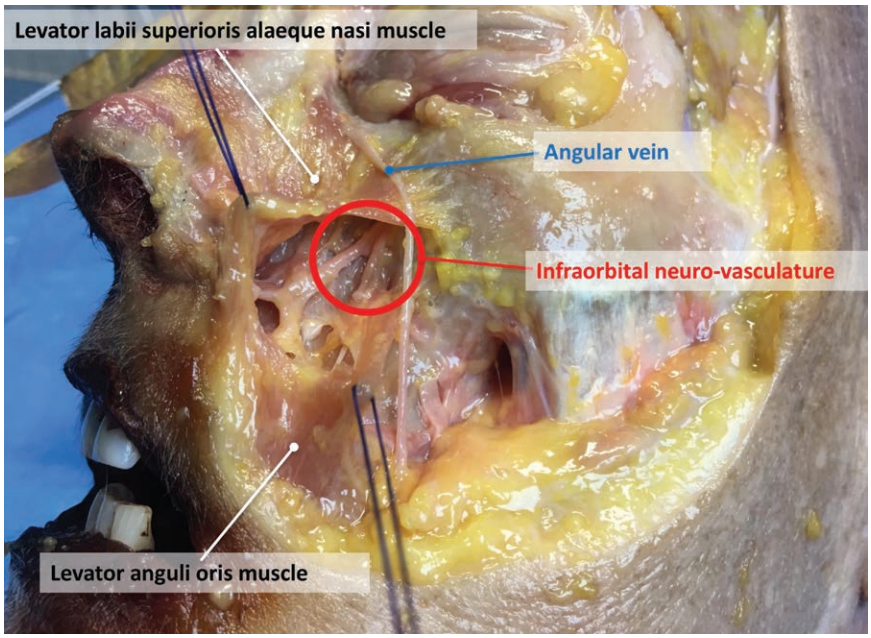

Fig. 6. Cadaveric dissection of the left face exposing the deep midfacial structures. Levator labii superioris alaeque nasi muscle, levator anguli oris muscle, angular vein, and infraorbital neurovascular bundle emerging from the infraorbital foramen.

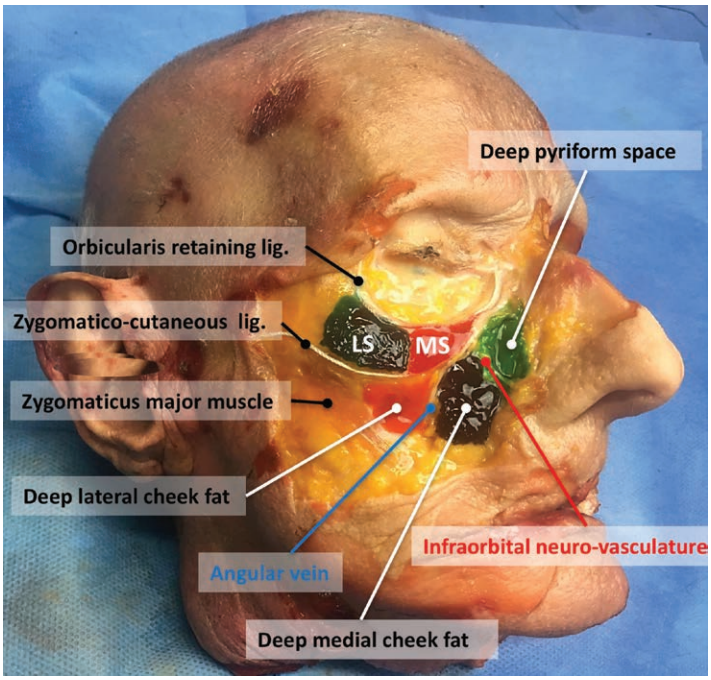

Fig. 7. Cadaveric dissection of the midfacial fat compartments with subsequent coloring of the deep facial fat compartments, for better illustration. The levator labii superioris muscle has been removed in this image to expose the deeper located fat compartments. *White ropes* indicate the location of the orbicularis retaining ligament and the zygomaticocutaneous ligament. *LS*, lateral sub–orbicularis oculi fat; *MS*, medial sub–orbicularis oculi fat. Note that the deep medial cheek fat is located between the angular vein (laterally) and the infraorbital foramen (medially).

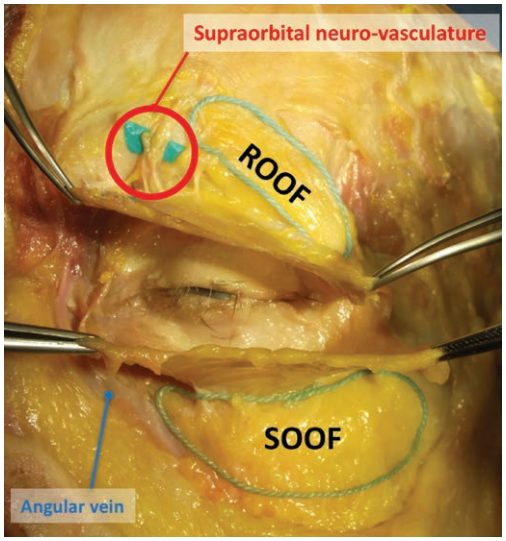

Fig. 8. Cadaveric dissections of the retro–orbicularis oculi fat (*ROOF*) and of the sub–orbicularis oculi fat (*SOOF*) after reflection of the orbicularis oculi muscle (held by the four pickup forceps in the image). Note that within the medial boundary of the sub–orbicularis oculi fat, the angular vein can be identified.

fat, located in the premaxillary space (r_p = –0.88; p = 0.021); here, no strong muscular or strong ligamentous structure forms the superior margin.

Deep Nasolabial Fat Located in the Premaxillary Space

The triangular deep nasolabial fat was identified within the premaxillary space, located superficial to the levator labii superioris alaeque nasi and deep to the orbital part of the orbicularis oculi muscle (its superior part) and by the midcheek superficial musculoaponeurotic system (SMAS) (its lower part). The medial wall is formed by the lateral nasal wall and the lateral nasal vein, whereas the lateral boundary is formed by a thin sheet of fibrous connective tissue covering the angular vein. The loose cranial boundary is formed likewise by the angular vein and its fascia, which runs inferior to the tear trough, whereas the inferior boundary is formed by the variable fascial fusion of the midcheek SMAS and the levator labii superioris

Table 1. Absolute Vertical and Horizontal Measures between the Horizontal Nasion Level and the Midline to the Most Superior/Inferior and Medial/Lateral Aspects of Each of the Investigated Deep Facial Fat Compartments

Compartment	Injected Volume ± SD (cc)	Vertical Distance to Inferior Aspect ± SD (mm)	Vertical Distance to Superior Aspect ± SD (mm)	Horizontal Distance to Medial Aspect ± SD (mm)	Horizontal Distance to Lateral Aspect ± SD (mm)	Correlation between Distance between Inferior Border of the Compartment and the Nasal Root and Injected Volume
Deep lateral cheek fat	0.66 ± 0.20	53.35 ± 4.98	33.99 ± 3.87	36.26 ± 3.87	53.61 ± 4.4	rp = 0.250; p = 0.459
Deep medial cheek fat	0.66 ± 0.27	52.56 ± 4.16	34.48 ± 3.29	23.72 ± 6.12	40.67 ± 6.27	rp = 0.291; p = 0.359
Deep nasolabial fat	0.76 ± 0.23	43.12 ± 7.02	17.4 ± 4.38	8.88 ± 1.79	23.75 ± 5.24	rp = −0.336; p = 0.514
Deep pyriform fat	0.81 ± 0.24	51.61 ± 4.72	30.88 ± 4.44	12.65 ± 4.77	25.28 ± 5.87	rp = −0.438; p = 0.089
Lateral SOOF	0.72 ± 0.29	35.85 ± 3.62	19.1 ± 3.97	40.45 ± 3.41	56.39 ± 3.2	rp = 0.329; p = 0.183
Medial SOOF	0.52 ± 0.27	40.44 ± 6.18	25.17 ± 2.73	23.74 ± 5.14	42.96 ± 4.89	rp = 0.262; p = 0.465

p, probability level; r_p, correlation coefficient from Pearson correlation analyses; SOOF, sub–orbicularis oculi fat.

alaeque nasi muscle (Tables 1 and 2 and Figs. 1 through 6).

The mean filling volume of this deep fat compartment was 0.76 ± 0.23, leading to a vertical extent of 25.72 ± 5.65 mm and to a horizontal extent of 14.87 ± 4.38 mm. No significant correlations were found between the volume of injected material and any change in the two-dimensional extent of this compartment (vertical, $p = 0.614$; horizontal, $p = 0.810$). Increased age also showed no significant relationship to any change in position (superiormost versus inferiormost boundary) or extent (vertical versus horizontal) of the compartment (all $p > 0.05$).

Deep Pyriform Fat Located in the Deep Pyriform Space

This deep fat compartment is located between the levator anguli oris and the levator labii superioris alaeque nasi muscle. It is bounded medially by the lateral nasal wall (in its superior part) and by the depressor septi nasi (in its inferior part). The lateral wall is formed by the fascial sheet surrounding the infraorbital neurovascular bundle (nerve, artery, veins) emerging from the infraorbital foramen, separating this fat compartment from the deep medial cheek fat. The inferior boundary is formed by the fusion of the levator labii superioris alaeque nasi and the levator anguli oris muscle at the level of the nasolabial sulcus, whereas the superior boundary is formed by the oblique (medial superior to lateral inferior) attachment of the levator labii superioris alaeque nasi muscle to the maxilla (Tables 1 and 2). The angular artery was found to course within this compartment (Figs. 1, 2, 4, 6, and 7).

The mean injected volume was 0.81 ± 0.24 cc and had a mean vertical/horizontal extent of 20.73 ± 3.37/12.63 ± 2.38 mm. No significant correlations were found between the amount of injected volume and the two-dimensional extent of the compartment (vertical, $p = 0.497$; horizontal, $p = 0.400$). Increased age also showed no significant relationship to any change in either the position (superiormost versus inferiormost boundary) or the extent (vertical versus horizontal) of the compartment (all $p > 0.05$).

Deep Medial Cheek Fat Located in the Deep Medial Cheek Fat Compartment

The deep medial cheek fat was located between the levator anguli oris and the levator labii superioris alaeque nasi muscle and thus in the same plane as the deep pyriform fat compartment. The medial boundary was formed by the fascial sheet surrounding the infraorbital neurovascular bundle emerging from the infraorbital foramen including the infraorbital nerve, artery, and veins, whereas the lateral boundary was formed by a thin sheet of connective tissue enclosing the angular vein. The superior boundary was formed by the bony attachment of the levator labii superioris alaeque nasi muscle, and the inferior boundary was formed by the fusion of the levator anguli oris and the levator labii superioris alaeque nasi muscle in its medial part and by the zygomaticus major and the transverse facial septum in its lateral part (Table 3 and Figs. 1 through 7).

Table 2. Current Description in the Literature of the Boundaries of the Premaxillary and Deep Pyriform Space and the Identified Boundaries Based on the Results of the Present Investigation

	Premaxillary Space		Deep Pyriform Space	
Border	**Literature**	**Proposal**	**Literature**	**Proposal**
Superior	Tear trough ligament[12]	Angular vein	—	Bony attachment of the levator labii superioris alaeque nasi muscle
Inferior	Pair of broad, transversely orientated retaining ligaments[12]; superior fornix of the oral mucosa[13]	Fascial fusion of the midcheek SMAS and the levator labii superioris alaeque nasi muscle	—	Levator anguli oris muscle
Medial	Nasal sidewall, levator labii superioris alaeque nasi and nasalis muscle[12]; canine fossa of the maxilla[13]	Lateral nasal wall and lateral nasal vein	Depressor septi nasi[8]	Lateral nasal wall and depressor septi nasi muscle
Lateral	Medial pupil line, is an area of loose areolar tissue approximately 5 mm[12]; buccomaxillary ligaments[13]	Angular vein	Deep medial cheek fat[8]	Infraorbital neurovascular bundle
Floor	Levator labii superioris muscle[12]; canine fossa of the maxilla[13]	Levator labii superioris alaeque nasi muscle	—	Levator anguli oris muscle and periosteum of the maxilla
Roof	Upper half of its roof is formed by the orbital part of the orbicularis oculi and the lower half is formed by the midcheek SMAS[12]	Orbital part of the orbicularis oculi muscle (in its superior part) and midcheek SMAS (in its lower part)	Deep medial cheek fat[8]	Levator labii superioris alaeque nasi muscle

Table 3. Current Description in the Literature of the Boundaries of the Deep Medial and Lateral Cheek Fat Compartments and the Identified Boundaries Based on the Results of the Present Investigation

	Deep Lateral Cheek Fat Compartment		Deep Medial Cheek Fat Compartment	
Border	**Literature**	**Proposal**	**Literature**	**Proposal**
Superior	—	Zygomaticocutaneous ligament and/or zygomaticus minor muscle	ORL[4,5,10]; oblique line of the maxilla[6]; zygomatic ligament[7]; zygomaticus major muscle[9]	Bony attachment of the levator labii superioris alaeque nasi muscle
Inferior	—	Zygomaticus major muscle and transverse facial septum	SOOF[10]; facial vein[7]	Fusion of the levator anguli oris and the levator labii superioris alaeque nasi muscle in its medial part and by the zygomaticus major and the transverse facial septum in its lateral part
Medial	Deep medial cheek fat pad[3]	Angular vein and deep medial cheek fat	Pyriform ligament[5,10]; lateral wall of the nose[6]; facial vein[7]; levator anguli oris[9]; pyriform and ORL[4]	Infraorbital neurovascular bundle
Lateral	Buccal fat pad[3]	Zygomaticus major muscle and transverse facial septum	Zygomaticus major and buccal fat pad capsule[6,10]; zygomaticus major[9]; maxilla[5]	Angular vein and deep lateral cheek fat
Floor	—	Periosteum of the maxilla	Periosteum of the maxilla[5,10]; Ristow space[6]; levator labii superioris[7]; levator anguli oris[9]	Periosteum of the maxilla
Roof	Superficial medial cheek fat pad[3]	Orbicularis oculi muscle and the midcheek SMAS	Subcutaneous medial and middle cheek fat compartment[5,10]; orbicularis oculi muscle[4] and SMAS[7]; alar crease[9]	Levator labii superioris alaeque nasi muscle

ORL, orbicularis retaining ligament; SOOF, sub–orbicularis oculi fat.

The mean injected volume was 0.66 ± 0.27 cc and the mean vertical/horizontal extent was 18.08 ± 4.07/16.95 ± 4.35 mm. No significant correlations were found between the amount of injected volume and the two-dimensional extent of the compartment (vertical, $p = 0.904$; horizontal, $p = 0.112$). Increased age also showed no significant relationship to a change in the position (superiormost versus inferiormost boundary) or the extent (vertical versus horizontal) of the compartment (all $p > 0.05$).

Deep Lateral Cheek Fat Located in the Deep Lateral Cheek Fat Compartment

The inverted triangular deep lateral cheek fat overlies the area around the zygomaticomaxillary suture and is in direct contact with the bone. The superior boundary is formed by

the zygomaticocutaneous ligament and/or the zygomaticus minor muscle (if present), whereas the medial boundary is formed by a thin layer of connective tissue enveloping the angular vein. The lateral and inferior boundary is formed by the zygomaticus major muscle and the transverse facial septum. The anterior boundary is formed by the orbital part of the orbicularis oculi muscle and the midcheek SMAS. This compartment had no connections to the buccal fat pad (located in the masticator space) or to the fat located within the buccal space (Table 3 and Figs. 1, 2, 5, and 7).

The mean injected volume was 0.65 ± 0.20 cc and the mean vertical/horizontal extent was 19.36 ± 3.29/17.36 ± 6.15 mm. No significant correlations were found between the amount of injected volume and the two-dimensional extent of the compartment (vertical, $p = 0.832$; horizontal, $p = 0.182$). Increased age showed no significant relationship to any change in position (superiormost versus inferiormost boundary) or extent (vertical versus horizontal) of the compartment (all $p > 0.05$).

Sub–Orbicularis Oculi Fat Located in the Sub–orbicularis oculi fat Compartment

In 100 percent of the investigated cases, the sub–orbicularis oculi fat was divided into two separate compartments: medial and lateral. The superior boundary is the bilaminar orbicularis retaining ligament, and the inferior boundary is formed by the zygomaticocutaneous ligament and/or the zygomaticus minor muscle (if present). The medial boundary extends until a vertical line passing through the medial margin of the pupil and is not connected to the tear trough area. The angular vein is embedded in the medial boundary, and the vein courses inferior to the tear trough toward the medial canthus. The lateral boundary is open and connected by means of the temporal tunnel to the inferior temporal compartment. This passage is superiorly framed by the lateral orbital thickening and inferiorly by the McGregor patch—the starting point of the zygomaticocutaneous ligament. The sub–orbicularis oculi fat lies on a thin sheet of fibrous connective tissue that is the midfacial extension of the superficial lamina of the deep temporal fascia and is thus separated from the prezygomatic space, which lies deep to this fat compartment (between fascia and periosteum) (Table 4 and Figs. 1, 2, 7, and 8).

The mean injected volume was 0.52 ± 0.27 cc for the medial sub–orbicularis oculi fat and 0.72 ± 0.29 cc for the lateral sub–orbicularis oculi fat. The maximal vertical/horizontal extent was 15.27 ± 5.20/19.22 ± 4.69 mm for the medial sub–orbicularis oculi fat and 16.74 ± 3.61/15.95 ± 3.25 mm for the lateral sub–orbicularis oculi fat. No significant correlations were found between the amount of injected volume and the two-dimensional extent of the compartment for the medial sub–orbicularis oculi fat (vertical, $p = 0.092$; horizontal, $p = 0.440$) or the lateral sub–orbicularis oculi fat (vertical, $p = 0.564$; horizontal, $p = 0.154$). Once again, increased age was not related to a change in position (superiormost versus inferiormost boundary) or to an increase in extent (vertical versus horizontal) of the compartment (all $p > 0.05$).

DISCUSSION

The results of this study summarize and expand the current understanding of the deep midfacial fat compartments and provide information on their precise anatomical location. Furthermore, the study describes comprehensively the boundaries of the deep midfacial fat compartments based on computed tomographic and magnetic resonance imaging accompanied by anatomical dissections: deep pyriform, deep medial cheek, deep lateral cheek, deep nasolabial (located within the premaxillary space), and the medial and lateral sub–orbicularis oculi fat. The results reveal that the location, when estimated by the position of the inferiormost and superiormost aspects of each of the visualized compartments, is not influenced by age or by the amount of injected material. No significant increase in the two-dimensional extent (vertical versus horizontal) was detected when various amounts of material were injected or with increased age.

In our opinion, the strengths of this study are the large sample size (40 fresh frozen cephalic specimens); the upright positioning of the cephalic specimen during computed tomographic imaging, simulating the effects of gravity; and the precise visualization of each of the midfacial deep fat compartments combined with anatomical dissections. Because of the injection of colored material during the imaging process, a direct comparison was possible in the consequent anatomical dissections. Doing so, the anatomical boundaries were identifiable and thus comparisons to the current descriptions in the literature were possible (Tables 2 through 4). However, a limitation of the presented results is that the study was carried out in cadaveric specimens, which lack systolic blood pressure and muscular activity of the facial and masticatory muscles, both of which are able to potentially contribute to a displacement and/or

Table 4. Current Description in the Literature of the Boundaries of the Medial and Lateral Sub–Orbicularis Oculi Fat Compartment and the Identified Boundaries Based on the Results of the Present Investigation

Border	Medial Sub–Orbicularis Oculi Fat Compartment		Lateral Sub–Orbicularis Oculi Fat Compartment	
	Literature	Proposal	Literature	Proposal
Superior	Lateral orbital thickening[11]	Orbicularis retaining ligament	Lateral orbital thickening[11]	Orbicularis retaining ligament and lateral orbital thickening
Inferior	Tear trough[11]	Zygomaticocutaneous ligament and/or zygomaticus minor muscle	Buccal fat pad[3]; tear trough[11]	Zygomaticocutaneous ligament and/or zygomaticus minor muscle
Medial	Medial limbus[3]	Angular vein and tear trough	Medial SOOF[11]	Medial SOOF
Lateral	Lateral SOOF[11]	Lateral SOOF	Lateral canthus[11]	Open and connected by means of the temporal tunnel to the inferior temporal compartment
Floor	Periosteum of the maxilla[3]	Midfacial extension of the superficial lamina of the deep temporal fascia	Zygoma[3]	Midfacial extension of the superficial lamina of the deep temporal fascia
Roof	Subcutaneous nasolabial and medial cheek fat[3]	Orbicularis oculi muscle	Lateral orbital compartment and middle cheek fat[3]	Orbicularis oculi muscle

SOOF, sub–orbicularis oculi fat.

breakdown of the injected soft-tissue filler. These influencing factors were—because of the nature of this cadaveric study—not studied and thus no conclusion was drawn on this aspect.

Our results are in line with most of the previous descriptions of the deep facial fat compartments[3–13] and provide additional clarification, especially when incorporating the concept of the course of the angular vein.[27] Another strength of the present study is that we injected variable amounts of material to test the expansibility and the migratory potential of each of the investigated midfacial fat compartments. Interestingly, we found no significant influence of either age or the amount of volume injected on the vertical or horizontal displacement of the visualized material when measured by computed tomographic imaging. This is contradictory to a previous computed tomographic imaging investigation of nine fresh frozen cephalic specimens performed by Gierloff et al.[3] that reported that an inferior displacement of the midfacial fat compartments occurred in the range of 1.3 to 2.6 mm when comparing individuals aged 54 to 75 years to those aged 75 to 104 years. However, these results have to be interpreted with caution, as it is widely accepted that changes of the facial skeleton occur during facial aging,[20–26] and thus adjustments of facial measurements have to be included in the analyses because of these age-related alterations. The results of Gierloff et al.[3] were not adjusted to facial distances but were related to the inferior orbital rim. When comparing the values from the literature measuring the inferior displacement of the inferior orbital rim during aging, Richard et al.[28] reported 0.5 to 2.0 mm in individuals aged 55 to 65 years as compared to 18- to 30-year-old individuals when measured by multiplanar computed tomographic imaging. Pessa et al.[21] reported an inferior displacement of the inferior orbital rim of 9.3 to 10.6 mm in their study sample, ranging from 18 to 80 years of age. Comparing these results to the inferior displacement of the facial fat compartments reported previously,[3] similarities (1.3 to 2.6 mm versus 0.5 to 2.0 mm) can be observed, and their descent can be potentially related more to the changes of the facial skeleton than to the descent of the fat compartments themselves. To account for this effect, we adjusted our measurements to facial skeleton parameters [i.e., vertical measures adjusted to the midfacial height (distance from the nasion to the base of the nasal spine), and horizontal measures adjusted to the widest transverse cranial diameter]. Our results were able to show that in our investigated sample, the midfacial height decreases with advanced age (range, 50 to 100 years), providing support for the "concertina" effect previously postulated by Pessa at al.[26] This age-related change in bone could be responsible for the "secondary" sagging/shrinking phenomenon seen in the overlying soft tissues (i.e., the facial fat compartments) and contribute to the appearance of an aged face. Adjusting for facial skeleton parameters can potentially reveal the true functional anatomy of the deep midfacial fat compartments; based on the results of this investigation, these compartments do not seem to become displaced inferiorly relative to the bone during the aging process. Because the boundaries of the deep nasolabial, deep pyriform, deep medial cheek, and deep lateral cheek fat compartments are bounded by facial muscles (Tables 2

through 4), it is plausible that their location is closely related to the origin and length of these muscles. A previous magnetic resonance imaging study of 20 healthy Caucasian female subjects (16 to 30 years versus 60 to 70 years)[15] found no difference in muscle length, thickness, volume, or location of origin between the investigated age groups; this supports the findings of our present study—a "relative" stable location of the deep facial fat compartments.

Our results are in line with a previous report by Lambros,[29] which stated that in the upper midface, a vertical descent of skin and subcutaneous tissue is not necessarily a major component of aging; this was based on his observation of the stability of orbicularis oculi wrinkles and moles as the same individuals aged over a time interval of 10 to 50 years. We found that, independent of the volume injected (range, 0.30 to 1.50 cc), no inferior migration occurred in any of the investigated deep fat compartments; this indicates a stable position of the content of an injected compartment.

These results support current concepts of soft-tissue filler injections wherein deep implantation (i.e., in contact with the bone) provides support for the overlying structures, increases the projected volume in an anterior orientation, and induces a lifting effect of more inferiorly located facial soft tissues. This effect seems plausible as, during aging, a redistribution of fat from superficial fat to visceral fat occurs,[30–32] and there is a loss of total subcutaneous fat mass with consequent "deflated" fat compartments. Soft-tissue filler injections are thought to "reinflate" these volume-deficient compartments (among other effects) and to restore the youthful appearance of the face.

CONCLUSIONS

The results of this cadaveric study suggest that, after adjustment for age-related changes of the facial skeleton, no inferior displacement of the deep facial fat compartments occurs with increasing age, when disregarding systolic blood pressure and muscular activity. Increased injected volumes did not cause inferior displacement of the injected "filler" material. This emphasizes the importance of deep, supraperiosteal implantation soft-tissue fillers for the support of the overlying structures, anterior projection, and a lifting effect of adjacent tissues.

Sebastian Cotofana, M.D., Ph.D.
Albany Medical College
47 New Scotland Avenue, MC-135
Albany, N.Y. 12208
cotofas@amc.edu
Instagram: professorsebastiancotofana

ACKNOWLEDGMENTS

The imaging part of this study received funding from Q-Med AB, Sweden (grant number 15092016), and from MERZ Pharmaceuticals GmbH (grant number 13072015). The authors would like to thank Katharina Erlbacher for support in the imaging part of this study and Hema Sundaram, M.D., for guidance during discussions.

REFERENCES

1. American Society of Plastic Surgeons. 2016 Plastic Surgery Statistics. Available at: https://www.plasticsurgery.org/documents/News/Statistics/2016/plastic-surgery-statistics-full-report-2016.pdf. Accessed June 1, 2017.
2. Cotofana S, Fratila AA, Schenck TL, Redka-Swoboda W, Zilinsky I, Pavicic T. The anatomy of the aging face: A review. *Facial Plast Surg.* 2016;32:253–260.
3. Gierloff M, Stöhring C, Buder T, Gassling V, Açil Y, Wiltfang J. Aging changes of the midfacial fat compartments: A computed tomographic study. *Plast Reconstr Surg.* 2012;129:263–273.
4. Sadick N, Dorizas A, Krueger N, Nassar A. The facial adipose system: Its role in facial aging and approaches to volume restoration. *Dermatol Surg.* 2015;41(Suppl XXX1):S333–S339.
5. Ramanadham SR, Rohrich RJ. Newer understanding of specific anatomic targets in the aging face as applied to injectables: Superficial and deep facial fat compartments. An evolving target for site-specific facial augmentation. *Plast Reconstr Surg.* 2015;136(Suppl):49S–55S.
6. Wenjin W, Yun X, Ru-Lin H, et al. Facial contouring by targeted restoration of facial fat compartment volume: The midface. *Plast Reconstr Surg.* 2017;139:563–572.
7. Cotofana S, Schenck TL, Trevidic P, et al. Midface: Clinical anatomy and regional approaches with injectable fillers. *Plast Reconstr Surg.* 2015;136(Suppl):219S–234S.
8. Surek CK, Vargo J, Lamb J. Deep pyriform space. *Plast Reconstr Surg.* 2016;138:59–64.
9. Surek CC, Beut J, Stephens R, Jelks G, Lamb J. Pertinent anatomy and analysis for midface volumizing procedures. *Plast Reconstr Surg.* 2015;135:818e–829e.
10. Rohrich RJ, Pessa JE, Ristow B. The youthful cheek and the deep medial fat compartment. *Plast Reconstr Surg.* 2008;121:2107–2112.
11. Rohrich RJ, Arbique GM, Wong C, Brown S, Pessa JE. The anatomy of suborbicularis fat: Implications for periorbital rejuvenation. *Plast Reconstr Surg.* 2009;124:946–951.
12. Wong CH, Mendelson B. Facial soft-tissue spaces and retaining ligaments of the midcheek: Defining the premaxillary space. *Plast Reconstr Surg.* 2013;132:49–56.
13. Pilsl U, Rosmarin W, Anderhuber F. The premaxillary space: A location for filler injection? *Dermatol Surg.* 2014;40:301–304.
14. Gosain AK, Amarante MT, Hyde JS, Yousif NJ. A dynamic analysis of changes in the nasolabial fold using magnetic resonance imaging: Implications for facial rejuvenation and facial animation surgery. *Plast Reconstr Surg.* 1996;98:622–636.
15. Gosain AK, Klein MH, Sudhakar PV, Prost RW. A volumetric analysis of soft-tissue changes in the aging midface using high-resolution MRI: Implications for facial rejuvenation. *Plast Reconstr Surg.* 2005;115:1143–1452; discussion 1153–1155.
16. Le Louarn C, Buthiau D, Buis J. Structural aging: The facial recurve concept. *Aesthetic Plast Surg.* 2007;31:213–218.

17. Wysong A, Kim D, Joseph T, MacFarlane DF, Tang JY, Gladstone HB. Quantifying soft tissue loss in the aging male face using magnetic resonance imaging. *Dermatol Surg.* 2014;40:786–793.
18. Wysong A, Joseph T, Kim D, Tang JY, Gladstone HB. Quantifying soft tissue loss in facial aging: A study in women using magnetic resonance imaging. *Dermatol Surg.* 2013;39:1895–1902.
19. Corey CL, Popelka GR, Barrera JE, Most SP. An analysis of malar fat volume in two age groups: Implications for craniofacial surgery. *Craniomaxillofac Trauma Reconstr.* 2012;5:231–234.
20. Richard MJ, Morris C, Deen BF, Gray L, Woodward JA. Analysis of the anatomic changes of the aging facial skeleton using computer-assisted tomography. *Ophthalmic Plast Reconstr Surg.* 2009;25:382–386.
21. Pessa JE, Chen Y. Curve analysis of the aging orbital aperture. *Plast Reconstr Surg.* 2002;109:751–755; discussion 756–760.
22. Kim SJ, Kim SJ, Park JS, Byun SW, Bae JH. Analysis of age-related changes in Asian facial skeletons using 3D vector mathematics on picture archiving and communication system computed tomography. *Yonsei Med J.* 2015;56:1395–1400.
23. Shaw RB Jr, Kahn DM. Aging of the midface bony elements: A three-dimensional computed tomographic study. *Plast Reconstr Surg.* 2007;119:675–681; discussion 682–683.
24. Pessa JE. An algorithm of facial aging: Verification of Lambros's theory by three-dimensional stereolithography, with reference to the pathogenesis of midfacial aging, scleral show, and the lateral suborbital trough deformity. *Plast Reconstr Surg.* 2000;106:479–488; discussion 489–490.
25. Farkas JP, Pessa JE, Hubbard B, Rohrich RJ. The science and theory behind facial aging. *Plast Reconstr Surg Glob Open* 2013;1:1–8.
26. Pessa JE, Zadoo VP, Yuan C, et al. Concertina effect and facial aging: Nonlinear aspects of youthfulness and skeletal remodeling, and why, perhaps, infants have jowls. *Plast Reconstr Surg.* 1999;103:635–644.
27. Cotofana S, Steinke H, Schlattau A, et al. The anatomy of the facial vein: Implications for plastic, reconstructive, and aesthetic procedures. *Plast Reconstr Surg.* 2017;139:1346–1353.
28. Richard MJ, Morris C, Deen BF, Gray L, Woodward JA. Analysis of the anatomic changes of the aging facial skeleton using computer-assisted tomography. *Ophthalmic Plast Reconstr Surg.* 2009;25:382–386.
29. Lambros V. Observations on periorbital and midface aging. *Plast Reconstr Surg.* 2007;120:1367–1376; discussion 1377.
30. Sepe A, Tchkonia T, Thomou T, Zamboni M, Kirkland JL. Aging and regional differences in fat cell progenitors: A mini-review. *Gerontology* 2011;57:66–75.
31. Palmer AK, Kirkland JL. Aging and adipose tissue: Potential interventions for diabetes and regenerative medicine. *Exp Gerontol.* 2016;86:97–105.
32. Lakowa N, Trieu N, Flehmig G, et al. Telomere length differences between subcutaneous and visceral adipose tissue in humans. *Biochem Biophys Res Commun.* 2015;457:426–432.